scientific reports

Check for updates

OPEN

Sources, seasonal trends and urban exposure to airborne particulate matter-bound pollutants

Anja Ilenič[1,2]✉, Radmila Milačič Ščančar[2,3], Alenka Mauko Pranjić[1], Nina Zupančič[4,5], Marija Đurić[1] & Janez Ščančar[2,3]

Size-fractionated airborne particulate matter was collected over 1 year (2023–2024) at five urban pedestrian and cycling locations in Slovenia. PM_{10}, $PM_{2.5}$, $PM_{0.1}$ were collected using a low-volume sampler with polytetrafluoroethylene filters, and $PM_{<0.1}$ fraction was retained in ultrapure-water. Metal(loid)s and polycyclic aromatic hydrocarbons (PAHs) were determined to assess the potential health and environmental risks. Metal(loid) concentrations were the highest in PM_{10}, with most elevated levels of Zn (7 ng m^{-3}), Ba (4.5 ng m^{-3}), Cu (2.8 ng m^{-3}) and Cr (1.5 ng m^{-3}). Significant enrichment in $PM_{<0.1}$ was observed for Ba, Cu, Ni, Pb and Zn, with Ce-normalised values indicating a strong anthropogenic contribution. Tailpipe tracers were dominant in (ultra)fine PM fractions, while non-exhaust emission markers (Ba, Cu, Zn) strongly correlated with Ce and La in PM_{10}. Among PAHs, BbF (0.05 ng m^{-3}), BghiP and IP (0.04 ng m^{-3}) exhibited the highest concentrations. BaP, BghiP and IP were enriched in ultra-fine particles, indicating fresh vehicular combustion emissions. Peak pollutant concentrations occurred during the heating period (HP) and in densely populated, high-traffic cities. Source apportionment revealed a dominance of pyrogenic sources, including: (i) vehicular exhaust emissions from diesel engines (5–6-ring PAHs, Ni, V and Pb), (ii) resuspended mineral dust and non-exhaust traffic particles (Ba, Cu, Zn), and (iii) coal and biomass combustion during HP (4-ring PAHs, Co, Mo, Tl). Incremental lifetime cancer risk for As (2×10^{-7}), Co (1×10^{-6}) and Cr (6×10^{-6}) was minimal. Hazard quotient values were below 1. Children cycling during HP experienced the highest exposure levels. The European PM_{10} limit values for As (6 ng m^{-3}), Cd (5 ng m^{-3}), Pb (500 ng m^{-3}), Ni (20 ng m^{-3}) and BaP (1 ng m^{-3}) were not exceeded.

Keywords Size-fractionation, Particulate matter, Metal(loid)s, Polycyclic aromatic hydrocarbons, Sources, Health risk assessment

The health impacts of urban airborne particulate matter (PM) are significantly influenced by its size and chemical composition. The most detrimental effects are associated with particles smaller than 2.5 µm, which predominantly originate from anthropogenic sources[1–3]. Exposure to fine and ultrafine particles (UFP), which can penetrate deep into the respiratory system, has been linked to numerous adverse health effects, including chronic and acute respiratory and cardiovascular diseases, such as stroke and lung cancer, ultimately leading to reduced life expectancy[4–6]. These health risks are at least partially attributed to the toxic substances bound to PM, such as metal(loid)s and polycyclic aromatic hydrocarbons (PAHs). These highly persistent compounds tend to bioaccumulate and can induce oxidative stress, highlighting the importance of understanding their environmental distribution[7,8]. Certain metal(loid)s (e.g. Ba, Cu, Ti and Zn) are considered useful conservative indicators of particulate emission sources due to their high atmospheric stability[2,9]. In urban environments, they are associated with high-temperature combustion processes, motor vehicle emissions, tyre and break wear, as well as road dust. Their contributions vary depending on the location and meteorological conditions[8,9]. PAHs are semi-volatile organic compounds with fused ring structures containing at least two benzene rings[10]. They are formed through incomplete combustion processes or the pyrolysis of organic matter such as wood, coal, natural gas or oil[10,11]. In the atmosphere, PAHs partition into gaseous and particulate phases based on their volatility. Low-molecular-weight (LMW) PAHs (2–3 rings) partition in the gas phase, while high-molecular-

[1]Department of Materials, Slovenian National Building and Civil Engineering Institute, 1000 Ljubljana, Slovenia. [2]Jožef Stefan International Postgraduate School, 1000 Ljubljana, Slovenia. [3]Department of Environmental Sciences, Jožef Stefan Institute, 1000 Ljubljana, Slovenia. [4]Faculty of Natural Sciences and Engineering, University of Ljubljana, 1000 Ljubljana, Slovenia. [5]ZRC SAZU Ivan Rakovec Institute of Paleontology, 1000 Ljubljana, Slovenia. ✉email: anja.ilenic@zag.si

weight (HMW) PAHs (4 or more rings) in the particulate phase[10]. The carcinogenicity of PAHs increases with the molecular weight[10]. Understanding the relationship between the particle chemical composition and size is essential, yet the available data remains limited. Sampling stations are typically installed on buildings' rooftops, and therefore do not accurately reflect the local environments where commuters (e.g. pedestrians, cyclists) reside[8,9,12–14]. Moreover, most studies have focused on a single pollutant type, either organic or inorganic, in size-fractionated PM_{10} or $PM_{2.5}$[8,9,15]; therefore, research on the multi-pollutant chemical composition of nanoparticles (PM_1 or smaller) is limited[11,16,17]. There is a lack of reported scientific studies focusing on small- to medium-sized European cities, where pollution characteristics may differ from those observed in large metropolitan areas and where cycling-based commuting is relatively common[16–20]. Therefore, to address these gaps, the aim of this study was to advance the understanding of urban airborne size-fractionated PM and its association with the size-specific chemical composition. The particular emphasis was on the assessment of PM < 0.1 µm, in pedestrian and cycling microenvironments of small and medium-sized Slovenian cities. We present the results of 1 year monitoring study of selected metal(loid)s and PAHs bound to PM_{10}, $PM_{2.5}$, $PM_{0.1}$ and $PM_{<0.1}$, which include an assessment of seasonal and spatial variability, source apportionment and an evaluation of the health risk implications associated.

Materials and methods

Sampling sites and sample collection

The airborne size-fractionated PM was collected over a 1-year period, from 1 June 2023 to 30 June 2024, at five urban locations in Slovenia, distributed along a traverse from south-west to north-west. The sampling sites included three distinctive urban locations—Maribor (MB: 46.548294, 15.649047), Ljubljana (LJ: 46.033985, 14.518328) and Murska Sobota (MS: 46.661490, 16.151619)—one residential area—Dobrova (DB: 46.067450, 14.409407)—and one reference area, with minimal or negligible pollution,—Piran (PR: 45.517636, 13.568725) (Fig. 1). The study area includes small- to medium-sized European cities, where pollution characteristics may differ from those in large metropolitan areas and where cycling-based commuting is relatively common. Smaller cities generally have significantly lower atmospheric pollutant levels due to reduced traffic density and fewer emissions from industry and residential heating and cooling systems, while better ventilation promotes more efficient pollutant dispersion.

Dobrova (population: 100) is a roadside settlement situated on the western outskirts of Ljubljana, the capital of Slovenia (population: 293,000). Both sampling sites lie within the Sava River basin, surrounded by the hills of the Dinaric Alps. Maribor, Slovenia's second largest city (population: 114,000), is located in the Drava River basin. Murska Sobota (population: 19,000) is situated in the Pannonian-flat landscape, while Piran (population: 18,000) is a coastal sampling location.

The sampling setups were positioned at ground level, at an average human height (170 cm), and they were located within one metre of bicycle lanes. Monthly samples were collected using a low-volume sampling cascade system, consisting of two identical units, one for the determination of PM-bound metal(loid)s and

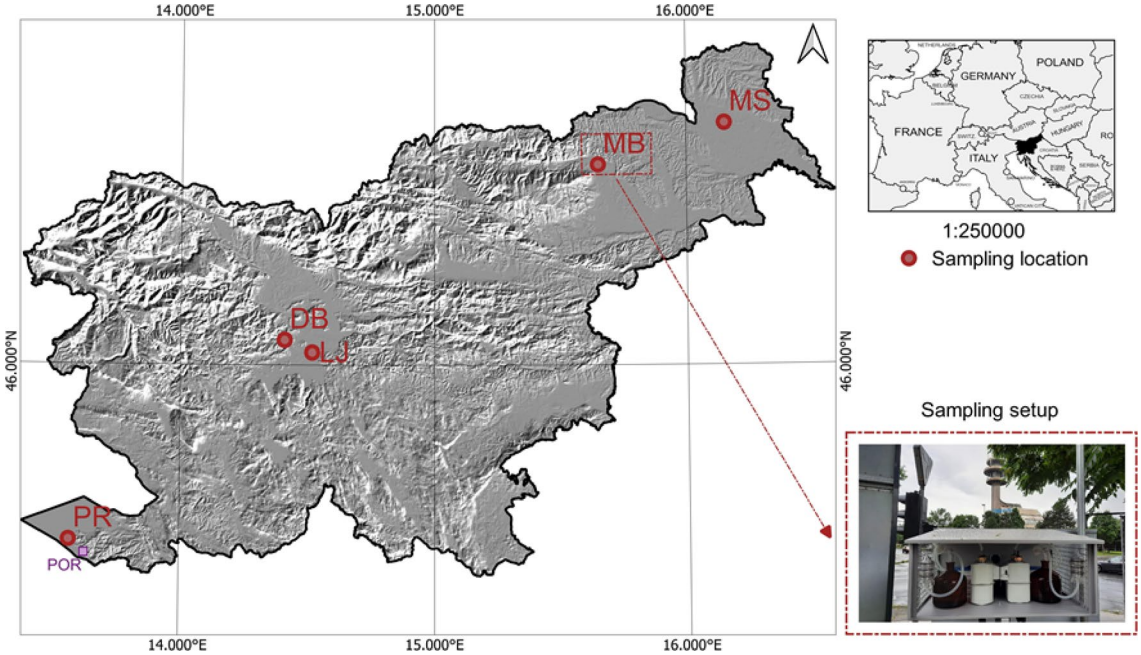

Fig. 1. Map of the study area showing sampling sites in Maribor (MB), Ljubljana (LJ), Murska Sobota (MS), Dobrova (DB) and Piran (PR). MB, LJ and MS represent urban areas, DB represents a residential area and PR a reference site. The map was created in QGIS software, using a digital relief model from the Geodetic Administration of the Republic of Slovenia (GURS) and the Slovenian Environmental Agency (ARSO), available at: https://gis.arso.gov.si/atlasokolja/profile.aspx?id=Atlas_Okolja_AXL@Arso.

the other for the determination of PM-bound PAHs. Each unit was equipped with a three-stage cascade polytetrafluoroethylene (PTFE) membrane filter holding system (Innovation NILU, Norway), incorporating hydrophobic filters with pore sizes of 10 µm, 2.5 µm and 0.1 µm (Mitex, Whatman, Omnipore; 47 mm diameter; Merck, KGaA, Darmstadt, Germany). The system was connected to an ultrapure-water trap (18.2 MΩ cm; Direct-Q 5 Ultrapure water system, PURELAB Flex 3, ELGA LabWater, UK) inside a 2000 mL amber glass burette bottle, used for collecting nanosized PM (< 0.1 µm). The airflow (approximately 11 L min^{-1}) passing through the system was controlled by a low-volume diaphragm pump (Vacuubrand ME 1 C; 100 mbar, 0.8 m^3 h^{-1}) connected to a gas meter (Dadolab Class G1.6 Laboratory dry gas meter, Italy). The airflow was monitored monthly throughout the entire sampling period, with an average airflow of 198 m^3 $month^{-1}$. Metal(loid) and PAH concentrations were reported in ng m^{-3} of air.

Analytical methods for characterising PM size-fractionated samples

A total of 480 size-fractionated airborne PM samples (PM_{10}, $PM_{2.5}$, $PM_{0.1}$, $PM_{<0.1}$) were collected (Tables S1–S9; Supplementary Information). Each PTFE filter (PM_{10}, $PM_{2.5}$, $PM_{0.1}$), along with $PM_{<0.1}$ retained in the ultrapure aqueous phase, represented the average monthly PM concentrations (Fig. 2). For the determination of metal(loid)s and PAHs, two consecutive monthly filters corresponding to each specific PM fraction at each sampling location were combined, yielding a total of 240 analyses. Prior to sampling, PTFE filters were pre-desiccated for at least 24 h and weighed (Mettler AE 163 analytical balance, Zürich, Switzerland) before and after PM collection to determine the precise proportion of the PM.

Determination of metal(loid)s in airborne size-fractionated PM

Arsenic (As), barium (Ba), cadmium (Cd), cerium (Ce), cobalt (Co), chromium (Cr), copper (Cu), lanthanum (La), molybdenum (Mo), nickel (Ni), lead (Pb), thallium (Tl), vanadium (V) and zinc (Zn) were determined in size-fractionated airborne PM using microwave-assisted acid digestion (Milestone Microwave Digestion System, Sorisole, Italy). A mixture of 3 mL nitric (HNO_3), 1 mL hydrochloric (HCl) and 0.2 mL hydrofluoric (HF) Suprapure acids was used. Prior to the total digestion, $PM_{<0.1}$ samples retained in the ultrapure aqueous phase were evaporated to 20 mL at 200 °C. Samples were then subjected to closed-vessel microwave-assisted digestion using the following temperature programme: ramp to 140 °C for 15 min, hold at 140 °C for 5 min, ramp to 200 °C for 20 min, hold at 200 °C for 60 min and cool down for 30 min. The clear digests were diluted to 30 mL with ultrapure water and the total elemental concentrations were determined by inductively coupled plasma mass spectrometry (ICP-MS, Agilent 7900 instrument, Agilent Technologies, Tokyo, Japan), using external calibration for quantification.

Determination of PAHs in airborne size-fractionated PM

The United States Environmental Protection Agency (US EPA) has identified 16 unsubstituted PAHs as priority pollutants, among which benzo(*a*)anthracene (BaA), benzo(*a*)pyrene (BaP), benzo(*b*)fluoranthene (BbF), benzo(*g*, *h*,*i*)perylene (BghiP), chrysene (Ch) and indeno(*1*,*2*,*3-cd*)pyrene (IP) are of particular concern due to their carcinogenic, teratogenic and mutagenic properties[21,22]. These compounds, along with fluoranthene

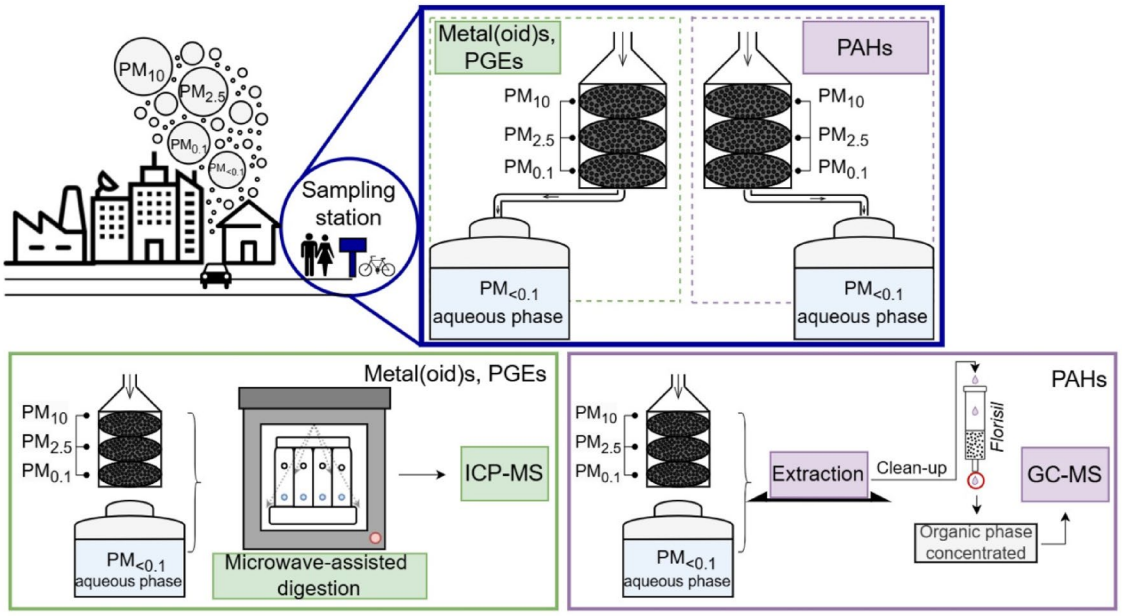

Fig. 2. Schematic presentation of the sampling device and analytical procedures for the determination of metal(loid)s, PGEs, and PAHs in size-fractionated airborne PM. Reproduced from Ilenič, A., Milačič Ščančar, R., Đurić, M., Mauko Pranjić, A., Ščančar, J. Analytical Methods, 2025, 17, 7184, with permission from the Royal Society of Chemistry.

(Fl) and pyrene (Pyr) were extracted from size-fractionated airborne PM using an organic solvent mixture of acetone (C_3H_6O) and petroleum ether (C_6H_{14}) (1:1, v: v), along with 2,2,4-trimethylpentane (C_8H_{18}) used as a retention agent. All samples were spiked with 50 µL of an internal standard (PAH-Mix 9 deuterated 10 µg mL^{-1} in cyclohexane). Extraction was performed by mechanical shaking (Vibromix 40 orbital shaker, Tehtnica, Železniki, Slovenia) at 180 rpm for 16 h. Extracts from $PM_{<0.1}$ retained in the ultrapure aqueous phase were then subjected to liquid-liquid extraction (LLE), followed by the removal of trace water with anhydrous sodium sulphate (Na_2SO_4, 550 °C, 6 h). The organic phase from both the filter extracts and the $PM_{<0.1}$ retained in the ultrapure aqueous phase was filtered through activated magnesium silicate (MgO_3Si; Strata FL-PR Florisil; 170 µm, 80 A, 500 mg^3 mL^{-1}; U.S. Silica Company) for sample clean-up and concentrated to approximately 1 mL under a nitrogen stream (N_2, 40 °C) using a sample concentrator (Dri-Block Heater DB100/3, Techne Inc., Vernon Hills, IL, USA). Finally, 1 µL of the concentrated sample was injected onto the column for PAH determination through gas chromatography mass spectrometry (GC-MS, Agilent HP6890; Mass selective detector 5973, Agilent Technologies, Tokyo, Japan), using external calibration for quantification.

Quality assurance and quality control

Prior to the analysis, the analytical procedures for determining metal(loid)s and PAHs were optimised using Standard Reference Material (SRM)® 1648a, Urban Particulate Matter, from the National Institute of Standards and Technology (NIST, USA); it was chosen for its matrix similarity and certified values for both analytes[23]. The repeatability of extraction methods for metal(loid)s[8,11,17] and PAHs[12] is rarely reported. Optimisation experiments were conducted in duplicate to evaluate the repeatability of measurements, limits of detection (LODs), limits of quantification (LOQs), linearity and accuracy. Measurement repeatability, calculated as the relative standard deviation (RSD), was evaluated using six replicate analyses of SRM 1648a. LODs and LOQs were estimated from six blank sample measurements, calculated as the concentrations corresponding to signals equal to 3*s* or 10 *s* of the blank samples with PTFE filter following microwave-assisted digestion. LODs ranged 0.001–0.23 ng mL for metal(loid)s and 4.5 ng mL for PAHs. The measurement repeatability and accuracy were 4% and 2% for selected metal(loid)s, and 3% and 6% for selected HMW PAHs. A spike recovery test was applied for elements not certified in SRM 1648a (Ba, Mo, Tl), with relative recoveries ranging from 92 to 107%.

Detailed and optimised analytical procedures along with quality assurance and quality control parameters are provided in Ilenič et al.[24].

Data analysis

The variability in the measured concentrations between different sampling sites (MB, LJ, MS, DB, PR), sampling seasons—non-heating period (NHP; March–October) and heating period (HP; November–February)—and PM size fractions (PM_{10}, $PM_{2.5}$, $PM_{0.1}$, $PM_{<0.1}$) were statistically analysed using parametric tests. Although the majority of the compound datasets were not strictly normally distributed, parametric test were used for reporting the results, due to higher statistical power of the method. This choice was justified by a large sample size and preliminary comparison between parametric and non-parametric tests, which yielded comparable outcomes at a significance level of $\alpha < 0.05$. The t-test and analysis of variance (ANOVA), and Pearson's correlation coefficients were applied to assess the relationship between variables, while cluster analysis using Ward's method as an amalgamation rule, 1-Pearson r as a distance measure for variables and the Euclidian distance for observations was used to identify natural groupings of the data. Prior to the analysis, outliers were removed and values below the LOD were replaced[25] with $LOD/\sqrt{2}$. Data analysis was conducted using TIBCO Statistica software[26], and the results were plotted using Origin[27]. Potential sources were identified through correlation analysis, diagnostic ratios (DRs), principal component analysis (PCA) on selected subsets of metal(loid)s or PAHs, separately. Parameter settings for the PCA included eigenvalues > 1.0, and results were presented as factor loadings, scree plots and correlations matrices to understand the relationship between different chemical species. Additionally, health risk assessment for residential exposure via inhalation was conducted.

Diagnostic ratios

DRs are a common conventional qualitative method for identifying potential sources of PAH pollution. The characteristic PAH ratios can be used to differentiate between contributions from various sources and are indicative of pyrogenic and petrogenic origins, as well as petroleum combustion sources (diesel or gasoline), biomass or coal burning and both traffic and non-traffic-related emissions, as these ratios remain constant between different emission sources[28–32]. DRs were calculated for each sampling location and PM size fraction. PAH concentrations below the LOD, specifically during NHP, were excluded from the analysis, and only ratios based on detectable values are reported.

Health risk assessment

The residential exposure of adults (female and male; 18–70 years old) and children (6 years old) to airborne PM-bound metal(loid)s and PAHs via inhalation was assessed through the calculation of the average daily dose (ADD, mg kg^{-1} day^{-1}), the incremental lifetime cancer risk (ILCR) and the hazard quotient (HQ). The assessment was conducted for each specific sampling site (MB, LJ, MS, DB, PR), PM size fraction (PM_{10}, $PM_{2.5}$, $PM_{0.1}$, $PM_{<0.1}$), activity type (cycling, walking), demographic group (male, female, child), sampling period (HP, NHP) and exposure scenario (normal, worst). The ADD (Eq. 1) for the respiratory pathway of metal(loid)s and PAHs was determined according to the following equation[33]:

$$\boldsymbol{ADD} = \frac{\boldsymbol{c_{air}} \times \boldsymbol{IR} \times \boldsymbol{ET} \times \boldsymbol{EF} \times \boldsymbol{ED}}{\boldsymbol{AT} \times \boldsymbol{BW}} \times 10^{-3} \quad (1)$$

where c_{air} represents the average measured concentration of the selected metal(loid) or PAH (in ng m^{-3}) bound to size-fractionated PM during a specific sampling period at a selected sampling site. *ED* represents the exposure duration, defined as 30 years for adults and 6 years for children, while *ET* refers to the average exposure time. In the normal-case scenario, *ET* reflects the average time an individual spends outdoors in Slovenia (1.8 h day^{-1}), whereas the worst-case scenario represents continuous 24 h day^{-1} exposure. *EF* is the exposure frequency (350 days $year^{-1}$), and *AT* is the total average exposure time over a lifetime (*ED* × 365)[34]. The inhalation rate (*IR*) varies by activity type and demographic group, where its respective values for men, women and children during cycling are 2.5 m^3 h^{-1}, 1.6 m^3 h^{-1} and 3.5 m^3 h^{-1}, respectively, and 0.8 m^3 h^{-1}, 0.5 m^3 h^{-1} and 1 m^3 h^{-1}, respectively, during walking[35]. The average body weight (*BW*) is assumed to be 85 kg for male adults, 68 kg for female adults and 32 kg for children[34].

The ILCR (Eq. 2) is defined as the incremental probability of an individual developing any form of cancer over their lifetime as a result of exposure to pollutants. The ILCR was determined according to the following equation:

$$ILCR = ADD \times IUR \tag{2}$$

IUR is the inhalation unit risk and is set for the following compounds[36]: As4.3 ng m^{-3}, Cd–1.8 ng m^{-3}, Co–9 ng m^{-3}, Cr–11 ng m^{-3}, Ni–0.26 ng m^{-3}, Pb–0.012 ng m^{-3}, BaA–0.06 ng m^{-3}, BaP–0.6 ng m^{-3}, BbF–0.06 ng m^{-3}, Ch–0.0006 ng m^{-3} and IP0.06 ng m^{-3}. ILCR greater than 10^{-4} indicates a potentially significant cancer risk, whereas ILCR below 10^{-6} suggests that the cancer risk from carcinogen exposure can be considered negligible. ILCR value of 10^{-6} corresponds to the probability that 1 in 1,000,000 individuals may develop cancer due to exposure to carcinogenic compounds[37].

The HQ (Eq. 3) reflects the probability of an individual experiencing an adverse effect and was calculated as follows:

$$HQ = \frac{ADD}{RfC} \tag{3}$$

where the chronic reference concentration (*RfC*) for metal(loid)s and PAHs is set as follows: As–15 ng m^{-3}, Ba–500 ng m^{-3}, Ce–900 ng m^{-3}, Cd–10 ng m^{-3}, Co–6 ng m^{-3}, Cr–30 ng m^{-3}, Mo2000 ng m^{-3}, Ni–10 ng m^{-3}, V–100 ng m^{-3} and BaP–2 ng m^{-3}. If the calculated HQ exceeds 1, adverse health effects could potentially be expected[35].

Meteorological conditions

The meteorological conditions were derived from monthly data collected between 2010 and 2016 for selected sampling locations (Table 1)[38]. The meteorological dataset does not coincide with the sampling period, potentially representing a study limitation. As concurrent meteorological data were not publicly available, the dataset presented in Table 1 was used to characterise the prevailing conditions and identify general, relatively stable patterns influencing air pollution, rather than short-term changes. As the locations Dobrova and Piran do not have national meteorological stations, data were sourced from the nearby locations—Ljubljana and Portorož (45.4753, 13.6160; see Fig. 1), respectively. The temperature (T) and relative humidity (RH) remain relatively stable at all locations. Ljubljana experiences the most rainfall, particularly during the HP. The wind speed (WS) and atmospheric pressure (P) are highest in Piran, the coastal sampling location, where SE winds prevail. In Maribor, P was not determined and is denoted as *nd*.

Location	Maribor	Ljubljana	Murska Sobota	Piran
HP				
T (°C)[a]	4.8 ± 3.0	5.1 ± 2.7	3.8 ± 3.3	8.3 ± 2.1
RH (%)[b]	75.8 ± 4.5	79.3 ± 3.9	81.8 ± 4.9	78.0 ± 3.2
TP (mm)[c]	63.5 ± 34.9	122 ± 47	60.1 ± 26.3	89.0 ± 36.8
P (hPa)[d]	*nd*	981 ± 4	993 ± 4	1015 ± 5
WS (m s^{-1})[e]	2.0 ± 0.2	1.1 ± 0.1	1.7 ± 0.3	2.6 ± 0.3
WD[f]	NW, SE	NE, N	N, E	SE
NHP				
T (°C)	16.4 ± 4.4	17.3 ± 4.7	16.9 ± 4.5	18.9 ± 4.7
RH (%)	74.0 ± 3.9	72.5 ± 5.5	74.6 ± 4.4	71.3 ± 3.7
TP (mm)	121 ± 67	181 ± 87	86.0 ± 47.9	121 ± 76
P (hPa)	*nd*	980 ± 3	993 ± 2	1014 ± 2
WS (m s^{-1})	2.2 ± 0.1	1.4 ± 0.4	1.9 ± 0.3	2.9 ± 0.3
WD	NW	NE	N, E	SE

Table 1. The meteorological conditions at various locations. [a]Temperature (T). [b]Relative humidity (RH). [c]Total precipitation (TP). [d]Atmospheric pressure (P). [e]Wind speed (WS). [f]Wind direction (WD)–NW (north-west), NE (north-east), N (north), E (east), SE (south-east). *nd* = not determined.

Results

Metal(loid)s distribution in airborne PM: size-fractions, seasonal and spatial trends

A total of 14 metal(loid)s (As, Ba, Ce, Cd, Co, Cr, Cu, La, Mo, Ni, Pb, Tl, V and Zn) were identified. The highest concentrations for most of the metal(loid)s were measured during the HP, while Ce, La, Ni and V showed elevated concentrations during the NHP (Figs. 3 and 4). As shown, the largest content of metal(loid)s was primarily concentrated in PM_{10}, with lower concentrations observed in $PM_{2.5}$ and $PM_{0.1}$. In the $PM_{<0.1}$ fraction, the concentrations of Ba, Cd, Cu, Ni and Zn reached levels comparable to those measured in PM_{10}. A strong anthropogenic contribution was confirmed with the normalisation to Ce and La. The average normalised ratios for Ba, Cr, Cu and Zn, as well as Ni and Pb were 82, 30, 38, 101, 12 and 7, respectively. The highest values were observed in the $PM_{<0.1}$ fraction. In urban environments, these metal(loid)s are commonly associated with exhaust and non-exhaust vehicular emissions[39]. Although PM_{10} fraction contained the highest content of selected metal(loid)s, the values observed for the ultra-fine fraction indicate on its importance, particularly for health considerations. Its small size and behavioural patterns similar to gas molecules enables deep penetration into lung tissue[40]. Despite their low total mass, UFPs can carry metal(loid)s more efficiently and enhance their reactivity and bioavailability. Consequently, UFPs may disproportionately contribute to overall human exposure via inhalation.

Metal(loid) concentrations were higher during the HP compared to NHP, with average HP-to-NHP ratios of 1.8, 2.1, 3.4 and 1.5 for PM_{10}, $PM_{2.5}$, $PM_{0.1}$ and $PM_{<0.1}$, respectively. The highest differences were observed for Co (ratio of 5.4), Mo (ratio of 3.1) and Tl (ratio of 6.5), with high correlations between Co and Mo, particularly in small PM fractions ($r = 0.9$), all typically associated with high-temperature fossil fuel combustion processes[41].

Furthermore, the full dataset for most metal(loid)s was non-normally distributed. When data were divided into subsets (particle size, location and season), the number of observations in each subset was relatively small. Nevertheless, both parametric ANOVA and non-parametric Kruskal–Wallis tests confirmed statistically significant differences ($p < 0.05$) for sampling locations, PM size fractions and seasons, with the PM size predominantly contributing the most to the overall variability.

Among the studied locations, the highest average levels of metal(loid)s were observed in Maribor, followed by Ljubljana, Murska Sobota, Dobrova and Piran. However, when compared by specific PM fraction, metal(loid) concentrations in PM_{10} were the highest in Maribor, while the pattern in finer fractions (below $PM_{2.5}$) was reversed and was the highest in Ljubljana. For comparison, Zn median concentrations in PM_{10} were 41.5 ng m^{-3} in Maribor and 6.1 ng m^{-3} in Ljubljana, while in $PM_{<0.1}$ they were 4.7 ng m^{-3} in Maribor and 9.2 ng m^{-3} in Ljubljana. A similar trend was observed for Ba, with median PM_{10} concentrations of 23.1 ng m^{-3} in Maribor and 5.3 ng m^{-3} in Ljubljana; and $PM_{<0.1}$ concentrations of 3.8 ng m^{-3} and 5.9 ng m^{-3}, respectively. For Ni, PM_{10} concentrations were 1.4 ng m^{-3} in Maribor and 0.5 ng m^{-3} for Ljubljana, whereas $PM_{<0.1}$ concentrations were 0.4 ng m^{-3} in Maribor and 0.8 ng m^{-3} in Ljubljana. These patterns are consistent with higher traffic density in Ljubljana and potentially greater influence of combustion-related sources.

Among the analysed elements, As, Cd, Pb and Ni have established annual threshold levels, with annual target values set for PM_{10} at 6 ng m^{-3}, 5 ng m^{-3}, 500 ng m^{-3} and 20 ng m^{-3}, respectively[42]. In this study, none of the target values were exceeded in any of the size-fractionated PM samples.

PAHs distribution in airborne PM: size-fractions, seasonal and spatial trends

A total of eight HMW PAHs were identified, including BaA (4-ring), BaP (5-ring), BbF (5-ring), BghiP (6-ring), Ch (4-ring), Fl (4-ring), IP (6-ring) and Pyr (4-ring). The highest concentrations of PAHs, in descending order, were observed for BbF, BghiP and IP, followed by Ch, BaP, Fl, Pyr and BaA. As shown in Fig. 5, the PAH concentrations were relatively low, ranging from 0.03 to 0.15 ng m^{-3}. The highest concentrations of HMW PAHs were associated with PM_{10}, $PM_{2.5}$ and $PM_{0.1}$, with total PAH sums of 3.4 ng m^{-3}, 1.1 ng m^{-3} and 1.6 ng m^{-3}, respectively. The highest mean concentrations of BaP, BghiP and IP were observed in the smallest PMs, attributed to greater surface area of $PM_{0.1}$ and association with fresh combustion origins. The spatial distribution of PAH concentrations exhibited a consistent trend across all locations, with the highest concentrations observed in Ljubljana (sum of PAHs equal to 2.9 ng m^{-3}), followed by Maribor (sum of PAHs equal to 1.7 ng m^{-3}), Dobrova (sum of PAHs equal to 1.3 ng m^{-3}) and Murska Sobota (sum of PAHs equal to 0.2 ng m^{-3}). No PAHs were detected in Piran or during the NHP at all locations. Generally, no statistically significant differences ($p > 0.05$) in HMW PAH concentrations were observed between different locations and PM size fractions. Seasonal variations contributed significantly to the overall variability. Among the analysed compounds, BaP is recognised as the most genotoxic carcinogen for humans, with an established annual threshold level[42] for PM_{10} set at 1 ng m^{-3}. In this study, BaP did not exceed the regulatory target at any location across all size-fractionated PM samples. The highest average BaP concentrations, equal to 0.11 ng m^{-3}, were measured in Ljubljana and Dobrova, most centrally located locations in Slovenia.

Discussion

Influence of meteorology on PM air pollution levels

Precipitation is considered one of the major meteorological factors influencing PM concentrations, primarily through wet deposition, which facilitates the removal of particles from the entire atmospheric column[43]. In Slovenia, precipitation increases from the coastal region (Piran) towards Ljubljana (NE), followed by a decrease towards the NE[44]. Another meteorological factor hindering effective air pollutant dispersion is a low wind speed (approximately 2 m s^{-1}, with the lowest values observed in LJ and MB). Elevated pollutant concentrations in Ljubljana and Maribor during the HP, result from unfavourable meteorological conditions, including a low WS, high RH and low T. Both locations are surrounded by hills and are susceptible to frequent thermal inversions due to the presence of a low planetary boundary layer level, a stable high-pressure system and the weak vertical

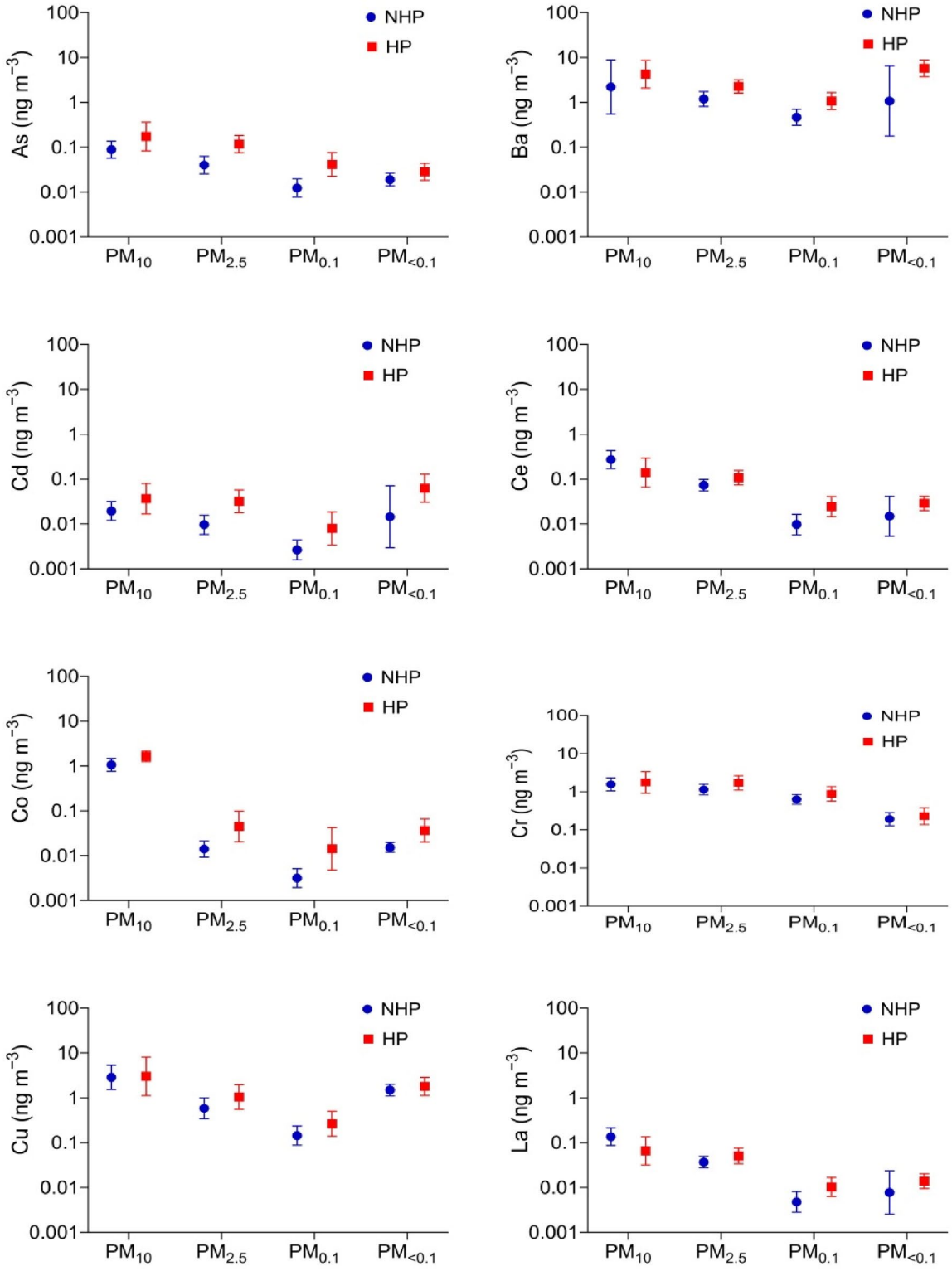

Fig. 3. Distribution of As, Ba, Cd, Ce, Co, Cr, Cu and La in size-fractionated airborne PMs. The non-heating period is denoted as NHP and the heating period is denoted as HP. The mean values with standard deviations are shown.

mixing of air masses in winter[45,46]. The presence of surrounding wetlands in Ljubljana can decrease the overall air pollution levels. Air masses originating from high-PM areas can increase air pollution levels in low-PM areas[45]. This pattern is likely contributing to the higher metal(loid) and PAH concentrations in Dobrova due to pollutant transport from Ljubljana, facilitated by NE winds (Table 1). Higher T during the NHP enhances

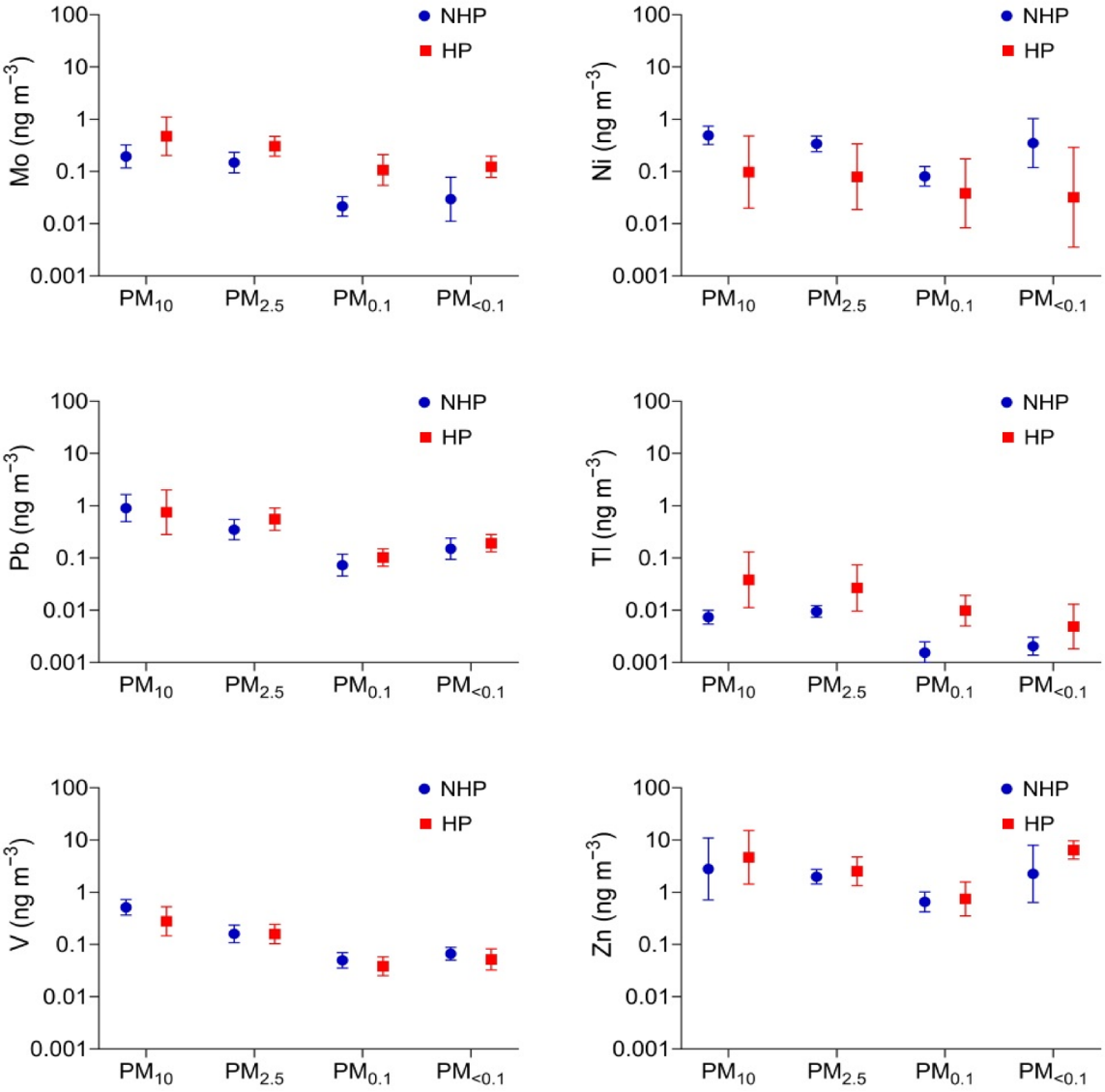

Fig. 4. Distribution of Mo, Ni, Pb, Ti, V and Zn in size-fractionated airborne PMs. The non-heating period is denoted as NHP and the heating period is denoted as HP. The mean values with standard deviations are shown.

HMW PAH photodegradation, reducing PAH concentrations in summer[47,48]. Additionally, dry surfaces and low wind speeds promote non-exhaust tracer resuspension, allowing submicronic particles to remain airborne longer[9]. Although precipitation alleviates airborne pollutant levels, its impact appears limited. Ljubljana, despite receiving the highest rainfall (115 mm in the NHP, 208 mm in the HP), still experiences the highest pollution levels. In addition, high ozone concentrations, especially in summer, can also significantly affect PAH levels and their degradation processes[48]. The average monthly ambient ozone levels during the NHP were approximately twice as high as those in the HP, with the highest concentrations recorded at the coastal sampling site Piran during the NHP, reaching 202 μg m^{-3} in June, also directly impacting on low PAH values (or values < LOD). Exceedances of the 120 μg m^{-3} target for 8-h observations were recorded at all locations[38,49].

Influence of emissions sources on PM air pollution levels

In this study, PCA, hierarchical clustering, ANOVA and Pearson correlation coefficient, along with DRs were employed for the source apportionment of selected metal(loid)s and HMW PAHs. The most dominant pyrogenic sources can be categorised into: (i) vehicular exhaust emissions, characterised by elevated concentrations of 5–6 HMW PAHs, Ni, V and Pb; (ii) particle ageing processes, mineral dust resuspension and non-exhaust emissions sources, dominated by significantly elevated concentrations of Ba, Cu and Zn; and (iii) coal and biomass combustion during HP, dominated by 4-ring PAHs, along with Co, Mo and Tl (Fig. 6).

The PCA of PAHs revealed two principal components explaining 96% of the total variance, with cluster analysis further grouping PAHs into: (i) BaP, BbF, BghiP, IP and Ch, and (ii) BaA, Pyr, Fl. High loadings of 5-

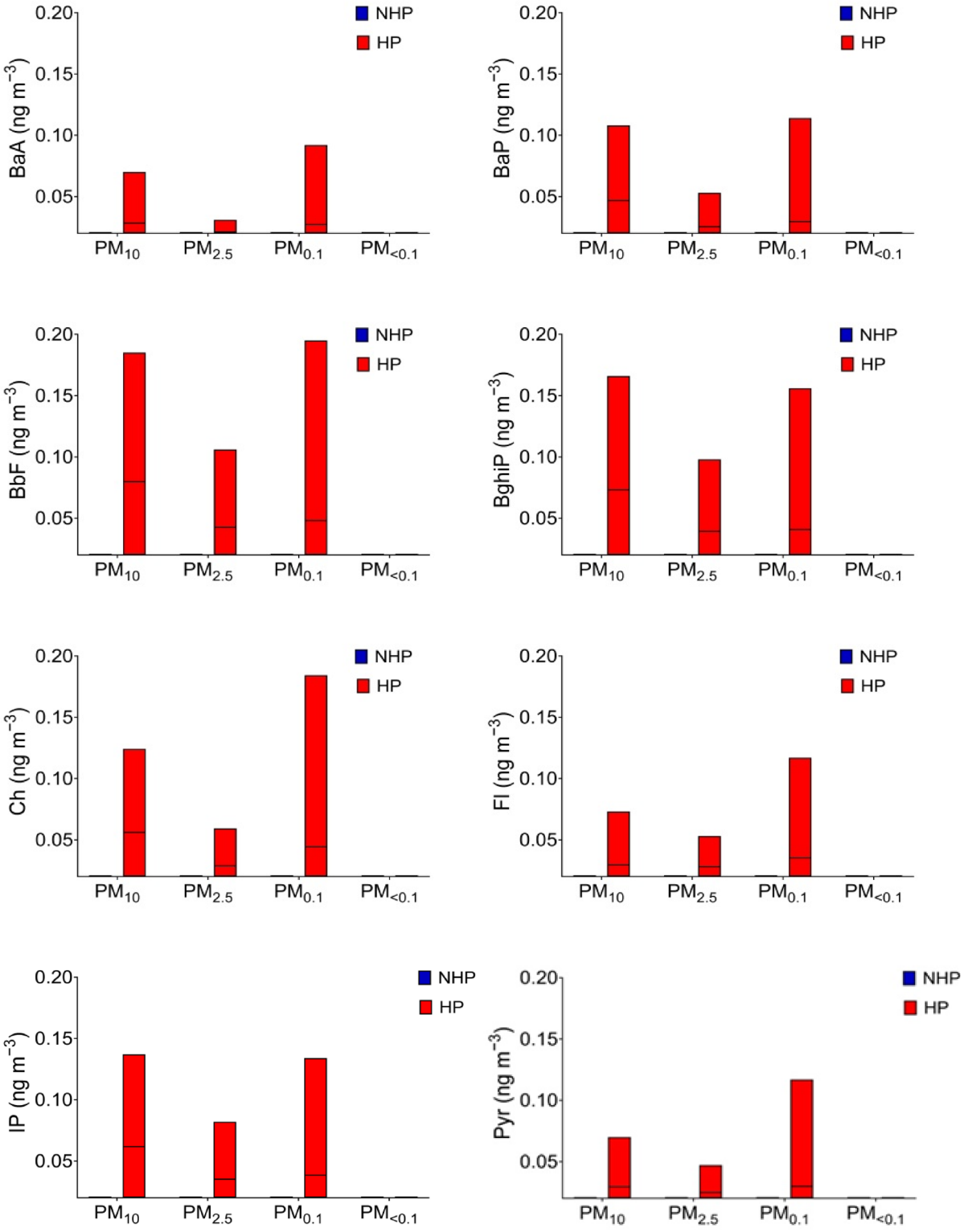

Fig. 5. Distribution of polycyclic aromatic hydrocarbons (PAHs) in size-fractionated airborne PMs. The non-heating period is denoted as NHP, and the heating period is denoted as HP. The mean values (lines) with ranges are shown.

and 6- HMW PAHs are indicative of high temperature combustion sources, while the second group suggests contributions from lower-temperature combustion processes, such as biomass and coal burning. HMW PAHs are, in comparison to LMW PAHs, more stable and less reactive to ozone oxidation and photodegradation processes; therefore, they serve as a reliable indicator of urban emission sources[50]. While differences in PAH

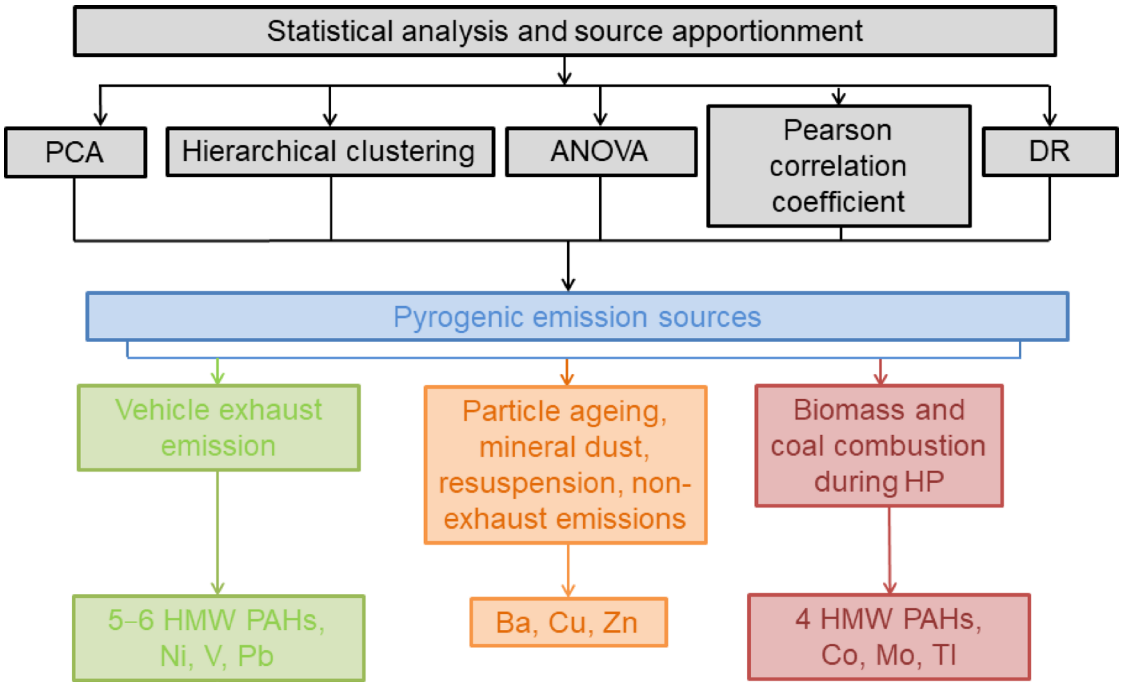

Fig. 6. Overview of the dominant pyrogenic emissions.

PAH ratio	DB	LJ	MB	MS	PR	Source	References
Fl/(Fl + Pyr)	0.51	0.57	0.51	*nd*	*nd*	Petrogenic: < 0.4	32
						Fossil fuel combustion: 0.4–0.5	
						Grass, wood, coal combustion: > 0.5	
BaA/(BaA + Ch)	0.33	0.30	0.36	*nd*	*nd*	Coal combustion: 0.2–0.35	28,32
						Vehicular emissions: > 0.35	
						Petrogenic: < 0.2	
						Combustion: > 0.35	
IP/(IP+BghiP)	0.43	0.47	0.46	0.47	*nd*	Petrogenic: < 0.2	32
						Petroleum combustion: 0.2–0.5	
						Grass, wood, coal combustion: > 0.5	
BaP/BghiP	0.47	0.61	0.66	*nd*	*nd*	Non-traffic emissions: < 0.6	30
						Traffic emissions: > 0.6	
IP/BghiP	0.75	0.89	0.86	0.89	*nd*	Gasoline: < 0.4	29
						Diesel: ~1	
BaP/(BaP + Ch)	0.41	0.41	0.47	*nd*	*nd*	Gasoline: ~0.73	31
						Diesel: ~0.5	

Table 2. PAH diagnostic ratios in size-fractionated PM at the various sampling locations with typical characteristic values. *nd* = not determined.

reactivity, volatility and solubility may introduce biases, DRs with similar physiochemical properties, derived from a specific formation mechanism, can serve as characteristic markers of major PAH sources[10,31]. Table 2 shows the DRs of the selected PAHs related to their respective sources. Certain isomeric PAH ratios in Murska Sobota and Piran were not determined (denoted as *nd*) due to PAH concentrations falling below the LOD. The calculated DRs indicate a dominance of pyrogenic sources, connected to exhaust and non-exhaust traffic emissions, primarily associated with the incomplete combustion of fossil fuels such as coal, oil and natural gas. In Maribor and Ljubljana, vehicular emissions—particularly from diesel engines, which represent 51% of the Slovenian fleet—appear to have a stronger influence compared to Dobrova, where PAH diagnostic ratios indicate non-traffic-related emission sources[51]. Diesel engines also emit significantly higher levels of PM compared to gasoline engines[52].

The presence of HMW PAHs is generally attributed to traffic emissions and biomass burning[15]. Consistent with findings from previous studies, DR in this study exhibited minimal variations between different PM size

fractions[28]. Additionally, the PAH ratio (3- and 4-ring PAHs)/(5- and 6-ring PAHs) serves as an indicator of the pollutant transport distance, with higher values suggesting longer-range transport[53]. The highest ratio was observed in Maribor (1.0), followed by Ljubljana (0.6), Dobrova (0.5) and Murska Sobota (0.3), indicating that air pollution sources in Murska Sobota are predominantly more localised.

In addition, comparability of PAHs across different PM fractions indicates a more homogenous source in comparison to metal(loid)s, also supported by a stronger correlation between PAHs and metals.

The PCA for metals revealed three principal factors, explaining 84% of the total variance. Dominating factors were categorised according to NHP and HP, resulting in three and two dominant components, respectively. During the NHP, Cd and Co differentiated from the other metal(loid)s, whereas during HP, three dominating factors were characterised as follows: (i) Cd, Co, Ni and Tl, (ii) Ba, Cu, Zn and (iii) all remaining analysed metal(loid)s. Additionally, elemental ratios are also used as fingerprints of specific anthropogenic emission sources. V/Ni ratio, typically reported in the range of 0.5–1.9, is indicative of gasoline and diesel vehicle combustion sources[54]. In this study, V/Ni ratios ($r = 0.9$) ranged from 0.1 to 1.2. The average values were 0.9 for PM_{10}, 0.6 for $PM_{2.5}$, 0.4 for $PM_{0.1}$ and 0.2 for $PM_{<0.1}$. Zn/Pb ratios ($r = 0.9$) exhibited higher values compared to those associated with traffic-related sources (< 1) reported by Prati et al.[55]. In this study, Zn/Pb ranged from 3.6 to 65.4, with average values of 6.7 for PM_{10}, 5.2 for $PM_{2.5}$, 9.1 for $PM_{0.1}$ and 27.5 for $PM_{<0.1}$. Cu, along with Ba and Zn, are considered well-established markers of non-exhaust emissions, particularly from tyre and brake wear[56]. These elements showed a strong linear relationship across all size-fractionated PM. Ba/Cu ratio ($r = 0.9$) varied between 0.6 and 9.2, with the highest values observed for $PM_{0.1}$ (3.5) and $PM_{<0.1}$ (3.6). The correlation coefficient was the highest in PM_{10} and decreased significantly in finer PM fractions, suggesting a greater contribution of road dust resuspension and mechanical abrasion debris to Cu compared to direct emissions. A similar pattern was observed for Zn/Cu ratio ($r = 1.0$), which varied between 0.7 and 6.9. The average values were 1.8 for PM_{10}, 2.9 for $PM_{2.5}$, 3.8 for $PM_{0.1}$ and 3.2 for $PM_{<0.1}$, with ratios higher than those found in the literature[57,58]. La/Ce ratio ($r = 1.0$) in this study ranged from 0.485 to 0.496 across different PM fractions, aligning with the typical crustal material value of 0.492. A decrease of La/Ce observed in $PM_{0.1}$ can indicate on an additional contribution of Ce from other sources, such as combustion. In addition, Ce and La showed stronger correlations with other metal(loid)s in the coarser PM fraction than in the finer fractions, indicating a potentially significant contribution of metal(loid)s associated with coarse PM fraction due to mechanical abrasion and resuspension processes. Pb/Cd ratio showed a wide range (1.1–95.2) and remained relatively constant across sampling sites, with the exception of MB, where a higher average value was recorded, indicating the localised enrichment of Pb sources connected to industrial activities[59]. Zn/Pb ratios ($r = 0.9$), varying from 3.6 to 65.4, were substantially elevated for $PM_{<0.1}$, further indicating on a strong influence of Zn sources in ultrafine particles. The elemental ratios remained constant between the NHP and HP, except for Pb/Cd. During the NHP, the average Pb/Cd ratio was 31.6, significantly higher than the values of 13.5 observed in the HP, suggesting enhanced contributions from traffic emission sources and resuspended dust outside the heating season. This was further supported by Pearson's correlations coefficients, with the highest correlation observed in coarser PMs, suggesting that Pb and Cd can be associated with particle aging and accumulation over time rather than with direct emission as ultrafine combustion particles.

A coefficient of variation (CV = 100 × standard deviation/mean) greater than 20% indicates a heterogeneous distribution in the environment[60]. In this study, Ba, Cd, Cu, Ni, Pb and Zn exhibited heterogeneous distributions across all locations, with the highest CV observed in Maribor (145%), followed by Dobrova (78%), Murska Sobota (75%), Ljubljana (73%) and Piran (72%). Among the particle size fractions, the CV associated with PM_{10} was the highest, followed by $PM_{0.1}$, $PM_{<0.1}$ and $PM_{2.5}$.

In Ljubljana and Maribor, key industries include energy production (power and heating plants), chemical manufacturing, metal processing and waste management. High differences observed for Co, Mo and Tl during HP compared to NHP, can be associated with high-temperature fossil fuel combustion processes[41]. Similar trends were observed in Poland and Germany, where HP levels were 2–3 times higher, mainly due to coal heating and poor dispersion conditions[9]. In Murska Sobota and Piran, key industries include tourism, food production (particularly meat processing) and metal manufacturing, with Piran having significant contributions from logistics and port operations. Across Slovenia, the primary contributors to PM_{10} and $PM_{2.5}$ are fuel use, traffic, agriculture and heat production[61]. In 2024, the majority of households (77%) had central heating (coal or wood biomass), and the most common primary heating sources were wood logs (30%), natural or propane gas (19%) and renewable sources (14%)[62,63]. In Slovenia, approximately 14% of households use local heating systems, in which each room is heated individually using stoves, fireplaces or electric heaters. About 9% of households are connected to district heating, where heat is supplied from a heating plant or central boiler[62]. In Maribor and Murska Sobota, the heating plants are located approximately 1.5 km from the sampling locations, whereas in Ljubljana the distance is about 3 km, which can potentially influence the local PM composition. In this study, the highest concentrations of 5- and 6-ring PAHs, including BbF, BghiP and IP, were detected across all locations. Typically, 3- and 4-ring PAHs are primarily emitted from coal combustion[64], and 4-, 5- and 6-ring PAHs are linked to vehicle emissions[10]; 5- and 6-ring PAHs are indicative of petroleum and oil combustion[10,64]. BaA, Ch, Fl and P are commonly used as tracers of coal combustion and biomass burning[12,65], while BaP, IP and BghiP are vehicle exhaust markers[13]. The highest correlation between PAHs and metal(loid)s was found for As ($r = 0.8$), especially in smaller PM sizes, indicating a similar origin. PAHs exhibited strong correlation also with Co, Cr, Mo and Tl. Among the metal(loid)s, the highest concentrations, in descending order, were observed for Zn, Ba, Cu, Cr and Pb. Ba, Cu, Cr and Zn, which are commonly associated with brake and wear tracers, were predominantly found in coarser PM[9,16,66,67]. In contrast, tailpipe tracers (e.g. Ni, Pb) were more prevalent in finer PM fractions[1,9,17,66]. It has also been reported that Co, Cd, Ni, Pb and Zn are linked to tyre wear, but Zn, Cr, Cu, Fe, Ba, Sb and Sn are more frequently connected with brake abrasion from road traffic[56].

Cross-study comparability of air pollution levels

Concentration ranges of metal(loid)s and PAHs were compared to other urban areas across the world (Table 3). The cross-study comparison highlights a significant gap in research addressing the chemical composition of UFPs, despite their high toxicity[68]. A review of studies published between 2010 and 2025 indicates that most of them predominantly focused on pollutants bound to $PM_{2.5}$ or PM_{10}, with only 5% assessing the chemical composition of UFPs. In addition, only 14% of the studies identified chemical composition of both pollutant groups within the single sampling campaign[68]. Therefore, this study provides important new findings.

Location	Metal(loid) (ng m^{-3})	Coarse PM	Fine PM	UFP PM	Ref.	Location	PAH (ng m^{-3})	Coarse PM	Fine PM	UFP PM	Ref.
Fez, Morocco	As Ba Co Cr Cu Pb Zn	0.03 28 31 35 27 36 156	/	/	69	Nanjing, China	BaP BbF BghiP Chr IP	/	0.5 2.5 0.7 1.5 0.6	/	13
Turin, Italy	As Cd Co Cr Cu Pb Zn	0.04–0.16 0–6 0.005–0.07 0.25–2.5 0.75–4.5 0.5–4.2 1–90	/	/	19	Delhi, India	BaP BbF BghiP Chr IP	7 3 2 4 2	10 4 4 6 3	/	70
Los Angeles, USA	Ba Co Cr Cu Pb Zn	26.2 0.11 1.1 12.1 0.9 9.2	25.7 0.09 2.0 12.8 2.2 11.5	/	71	Zagreb, Croatia	BaP BbF Chr BghiP IP	*nd*–29.27 *nd*–16.56 *nd*–13.78 *nd*–38.78 2.45–119	*nd*–27.2 *nd*–10.9 *nd*–11.1 *nd*–37.7 0.42–84	/	11
Žilina, Slovakia	As Ba Cd Cr Cu Pb Zn	0.4 14.1 0.0 1.7 19.5 1.7 14.2	0.7–2.2 1.9–2.1 0.1–0.5 0.9–1.2 5.8–10.5 3.8–13.7 22.1–72.5	/	16	Naples, Italy	BaP Chr IP	0.065–0.872 0.003–0.805 0.001–0.516	/	/	47
Leipzig, Germany	As Ba Co Cr Cu Pb Zn	0–7.7 0–20 0–1.2 0–5.9 0.14–50 0.02–48 1.1–171	/	/	9	Ankara, Turkey	BaP BbF BghiP Chr IP	/	2.46 5.34 1.48 3.07 4.65	/	72
Manlleu, Spain	As Ba Cd Co Cr Cu Pb Zn	0.9 17 0.7 0.1 6.1 73 24 124	/	/	73	Manlleu, Spain	BaP	1.5	/	/	73
Rome, Italy	As Cd Cr Cu Pb Zn	/	0.36–0.60 0.09–0.37 2.43–4.40 9.02–18.6 4.08–13.0 12.1–29.3	/	74	Giza, Egypt	BaP BbF BghiP Chr IP	/	0.55–78.75 *nd*–54.89 1.61–192.57 0.68–45.99 0.12–118.23	/	75
Katowice, Poland	As Cd Pb	/	1.38–3.68 0.49–2.92 22.92–83.46	/	20	Katowice, Poland	BaP	/	0.79–35.93	/	20
Thessaloniki, Greece	Cr Cu Pb Zn	/	*nd*–0.261 0.009–2.218 0.011–0.201 *nd*–4.126	/	76	Thessaloniki, Greece	BaP BbF BghiP Chr IP	/	*nd*–2.14 0.05–5.52 *nd*–2.66 *nd*–3.62, *nd*–3.92	/	76
This study	As Ba Cd Co Cr Cu Pb Zn	0.02–0.71 0.84–26.0 0.004–0.20 0.37–4.33 0.46–8.89 0.35–29.1 0.14–10.1 0.53–69.2	0.01–0.44 0.35–6.68 0.002–0.10 0.003–0.24 0.22–5.75 0.11–5.02 0.09–1.65 0.53–7.14	0.003–0.26 0.15–12.99 0.001–0.10 0.001–0.17 0.09–3.54 0.05–6.88 0.02–2.01 0.19–15.5	/	This study	BaP BbF BghiP Chr IP	< 0.02–0.11 < 0.02–0.18 < 0.02–0.17 < 0.02–0.12 < 0.02–0.14	< 0.02–0.05 < 0.02–0.11 < 0.02–0.10 < 0.02–0.06 < 0.02–0.08	< 0.02–0.11 < 0.02–0.20 < 0.02–0.16 < 0.02–0.18 < 0.02–0.13	/

Table 3. Metal(loid)s and PAHs concentration ranges across different urban locations. Ref. = reference, *nd* = not determined, / = not reported.

It was observed, that the metal(loid) concentrations in this study were significantly lower than those reported for larger cities, such as Fez, Morocco (population: 1.1 million), but similar to Žilina, Slovakia (population: 0.6 million) and Leipzig, Germany (population: 0.6 million). PAH distribution patterns were similar to those in Zagreb, Croatia (population 0.8 million) (Table 3), with the highest total PAH concentrations also observed during the HP[11]. Similarly low sums of PAHs (1–2.1 ng m^{-3} in PM_{10} and $PM_{2.5}$ were observed in Rome (Italy), Copenhagen (Denmark), London (United Kingdom) and Oslo (Norway)[15]. 5- and 6-ring PAHs prevailed across all studied locations, similar to Naples (Italy)[47]. PAHs with 4-, 5- and 6-rings exhibit lower vapour pressures, which favour their partitioning in PM[77]. The presence of HMW PAHs can be attributed to traffic emissions, as well as biomass burning[65]. Regarding other European cities, the highest BaP values were recorded in Athens (Greece) and Copenhagen (Denmark), with values of 0.25 ng m^{-3} and 0.21 ng m^{-3}, respectively[15]. In Zagreb (Croatia)[11], BaP values exceeded the regulatory threshold level of 1 ng m^{-3}. BaP values in Porto (Portugal) varied between 0.01 ng m^{-3} and 2.7 ng m^{-3}, with an average value 0.37 ng m^{-3}; meanwhile, the average BaP values were 0.25 ng m^{-3} in Athens and 0.21 ng m^{-3} in Copenhagen[15]. Similar trends across different cities confirm similar chemical fingerprinting, attributed to more localised emission sources in Slovenian cities, a higher traffic density per unit volume of air and the limited dispersion of air pollutants.

Potential health risk implications

Potential health risks associated with As, Cd, Co, Cr, Mo, Pb, V, BaA, BaP, BbF, Ch and Pyr (Tables S10–S13, Supplementary Information) were evaluated for both, typical exposure conditions (1.8 h day^{-1}, representing the average outdoor time in Slovenia)[34] and the worst-case scenario (24 h day^{-1} exposure), during the NHP and HP and for different size-fractionated PM. In this study, no ILCR or HQ values for the specific groups exceeded the recommended threshold levels[35,37]. However, some ILCR values were above 10^{-6}, in particular for As, Co, Cr, suggesting a minimal potential carcinogenic risk[37]. The highest exposure risk was observed for child cyclist exposed to Cr bound to PM_{10} during 24 h day^{-1} exposure in winter (6.6×10^{-5}), while an ILCR of 4.9×10^{-5} was observed under 1.8 h day^{-1} exposure. Elevated ILCR values (24 h day^{-1} exposure) for children were also noted for $PM_{2.5}$ (4.5×10^{-5}), $PM_{0.1}$ (2.3×10^{-5}) and $PM_{<0.1}$ (6.2×10^{-5}). Under normal exposure conditions (1.8 h day^{-1}), Cr ILCR values exceeded the 1×10^{-6} threshold in $PM_{2.5}$ (3.3×10^{-6}) and $PM_{0.1}$ (1.7×10^{-6}). For adults, Cr-related ILCR values also exceeded the threshold value in both exposure scenarios during cycling activity. Co-related ILCR values were of concern particularly under 24 h day^{-1} exposure in PM_{10} (2.0×10^{-6} to 3.3×10^{-5}), as well as in the normal-case scenario for children cycling (2×10^{-6}). As-related ILCR values were similarly elevated for children during cycling activities under 24 h day^{-1} exposure in PM_{10} (2×10^{-6}) and $PM_{2.5}$ (1×10^{-6}).

Overall, in both exposure scenarios, the most concerning metal(loid)s in PM_{10} were Cr, Co and As, with ILCR values of 2×10^{-6} and 2×10^{-5}, 8×10^{-7} and 1×10^{-5}, and 5×10^{-8} and 6×10^{-7}, respectively. Among the PAHs, BaP (1×10^{-9} and 1×10^{-8}, respectively), BbF (2×10^{-10} and 2×10^{-9}, respectively) and Pyr (8×10^{-11} and 1×10^{-9}, respectively) were considered most problematic. In $PM_{2.5}$, the highest ILCR values were calculated for Pb (1×10^{-6} and 1×10^{-5}, respectively), Cd (2×10^{-8} and 3×10^{-7}, respectively) and Cr (2×10^{-8} and 2×10^{-5}, respectively), as well as for Pyr (5×10^{-9} and 7×10^{-8}, respectively) and BaA (4×10^{-10} and 5×10^{-9}, respectively). In $PM_{0.1}$, the highest ILCR values were calculated for Ce (5×10^{-7} and 7×10^{-6}, respectively), Ni (1×10^{-8} and 1×10^{-7}, respectively) and Pb (9×10^{-9} and 1×10^{-7}, respectively), indicating a significant contribution of vehicular exhaust emissions. Among PAHs, Pyr (9×10^{-10} and 1×10^{-8}, respectively), BaP (1×10^{-10} and 1×10^{-9}, respectively) and Ch (8×10^{-11} and 1×10^{-9}, respectively) exhibited the highest ILCR values. In $PM_{<0.1}$, the highest ILCR values were calculated for As (2×10^{-7} and 2×10^{-6}, respectively), V (8×10^{-9} and 1×10^{-7}, respectively) and Ce (7×10^{-9} and 9×10^{-8}, respectively).

ILCR values were consistently higher during the HP compared to the NHP, ranging from 2×10^{-13} to 4×10^{-6} for the NHP, and from 1×10^{-13} to 5×10^{-6} for the HP. The highest average ILCR values were observed in MB and LJ, with values of 1×10^{-6} and 8×10^{-7}, respectively. Higher ILCR values were also observed during cycling activities (1×10^{-6}) compared to walking (3×10^{-7}); this is primarily attributed to the increased respiratory rates and greater volume of inhaled air associated with demanding physical activities. On average, cyclists experience three-times-higher levels of exposure to air pollution than pedestrians when subjected to the same exposure duration[78–80]. However, their calculated risk remain below the critical threshold level.

Additionally, the calculated HQ did not exceed the threshold level of 1, signifying minimal exposure risks for the observed compounds[35]. Similar to the ILCR values, HQ values were generally higher during the HP, with the highest levels observed in MB, followed by LJ, DB, MS and PR. Under the worst-case conditions, carcinogenic risk factors were markedly elevated, reflecting the same trend observed for ILCR values.

For comparison, the ILCR values reported in Seoul, South Korea[81], were relatively low, ranging from 5.6×10^{-6} to 7.5×10^{-6}. In Naples, Italy[47], PAH-related ILCR values for PM_{10} were negligible. The BaA-related ILCR was 2.1×10^{-7} for adults and 5.8×10^{-8} for children, respectively. The Chr-related ILCR was 2.7×10^{-10} for adults and 7.7×10^{-10} for children, while the BaP-related ILCR values were 4.8×10^{-7} for adults and 1.4×10^{-6} for children. The IP-related ILCR values were 1.6×10^{-8} for adults and 4.6×10^{-7} for children. In Zhengzhou and Beijing, China[8,45], elevated ILCR values and high concentrations of BaA, BaP, BbF, Pb, As, Cr, Cd and Ni were observed, particularly during the NHP.

Based on all health risk associated calculations, Cr exhibited the highest potential carcinogenic risk among the assessed metal(loid)s, while BaP posed the greatest risk among PAHs (Figs. 7 and 8).

Outdoor activities in Slovenia, especially in high-traffic areas and during periods of poor pollutant dispersion (winter), can pose potentially elevated health risks for certain demographic groups, such as children, cyclists and residents in the close proximity to traffic and/or heating sources. Reducing emissions, improving public awareness and implementing targeted urban planning, as well as stricter regulations are essential to lower overall exposure.

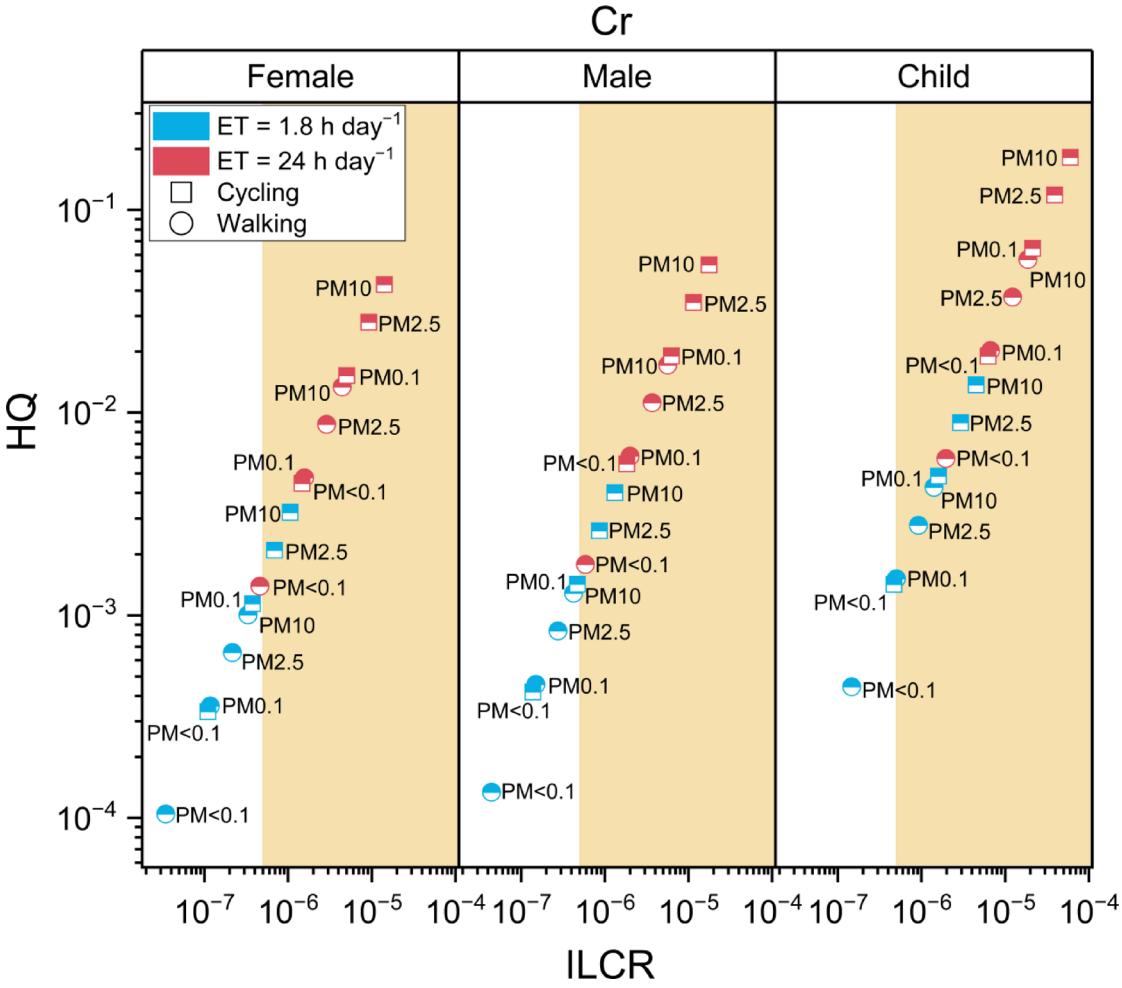

Fig. 7. The incremental lifetime cancer risk (ILCR) and hazard quotient (HQ) values associated with the inhalation of chromium (Cr).

Conclusions

Size-fractionated airborne PM-bound metal(loid)s and PAHs were determined in PM_{10}, $PM_{2.5}$, $PM_{0.1}$ and $PM_{<0.1}$, collected over 1 year at five pedestrian and cycling urban microenvironments in Slovenia.

The analysis revealed that the majority of metal(loid)s (e.g. Zn, Ba, Cu, Cr) reached peak concentrations during the heating period (winter), while Ce, La, V and Ni dominated during the non-heating period. The largest NHP-to-HP differences were observed for Co, Mo and Tl, metal(loid)s commonly associated with biomass and coal combustion processes. In the $PM_{<0.1}$ fraction, the concentrations of Ba, Cd, Cu, Ni and Zn reached levels comparable to those measured in PM_{10}, with Ce-normalised values indicating a strong anthropogenic contribution. Tailpipe tracers (Ni, V, Pb) were dominant in (ultra)fine PM fractions, while non-exhaust emission markers (tyre and break wear; Ba, Cu, Zn) strongly correlated with Ce and La in PM_{10}. The strongest correlations were observed between As, Co, Cr, Tl, Mo and PAHs, in particular in finer PM fractions, indicating a likely common source.

Total PAH sums were 3.4 ng m^{-3}, 1.1 ng m^{-3} and 1.6 ng m^{-3} for PM_{10}, $PM_{2.5}$ and $PM_{0.1}$, respectively, with BbF, BghiP and IP exhibiting the highest concentrations. BaP, BghiP and IP were enriched in UFPs, indicating fresh vehicular combustion emissions.

The highest HP concentrations occurred in densely populated Ljubljana and Maribor, resulting from frequent thermal inversions, low planetary boundary layer height and limited vertical air mixing, allowing submicronic particles to remain airborne longer.

Source apportionment indicated a dominance of pyrogenic sources, with elevated contributions from (i) vehicular exhaust emissions, primarily associated with diesel engines, and characterised by 5- and 6- PAHs as well as Ni, V and Pb (ii) particle ageing, mineral dust resuspension and non-exhaust emission sources, such as tyre and brake wear, marked by elevated concentrations of Ba, Ce, Cu, La and Zn; and (iii) coal and biomass combustion during the HP.

The calculated ILCR for pedestrians and cyclist among different demographic groups, indicated an overall negligible cancer risk, except for As (2×10^{-7}), Co (1×10^{-6}) and Cr (6×10^{-6}), which exhibited low potential risks through inhalation. The highest exposure levels were identified for children engaged in cycling activities in the

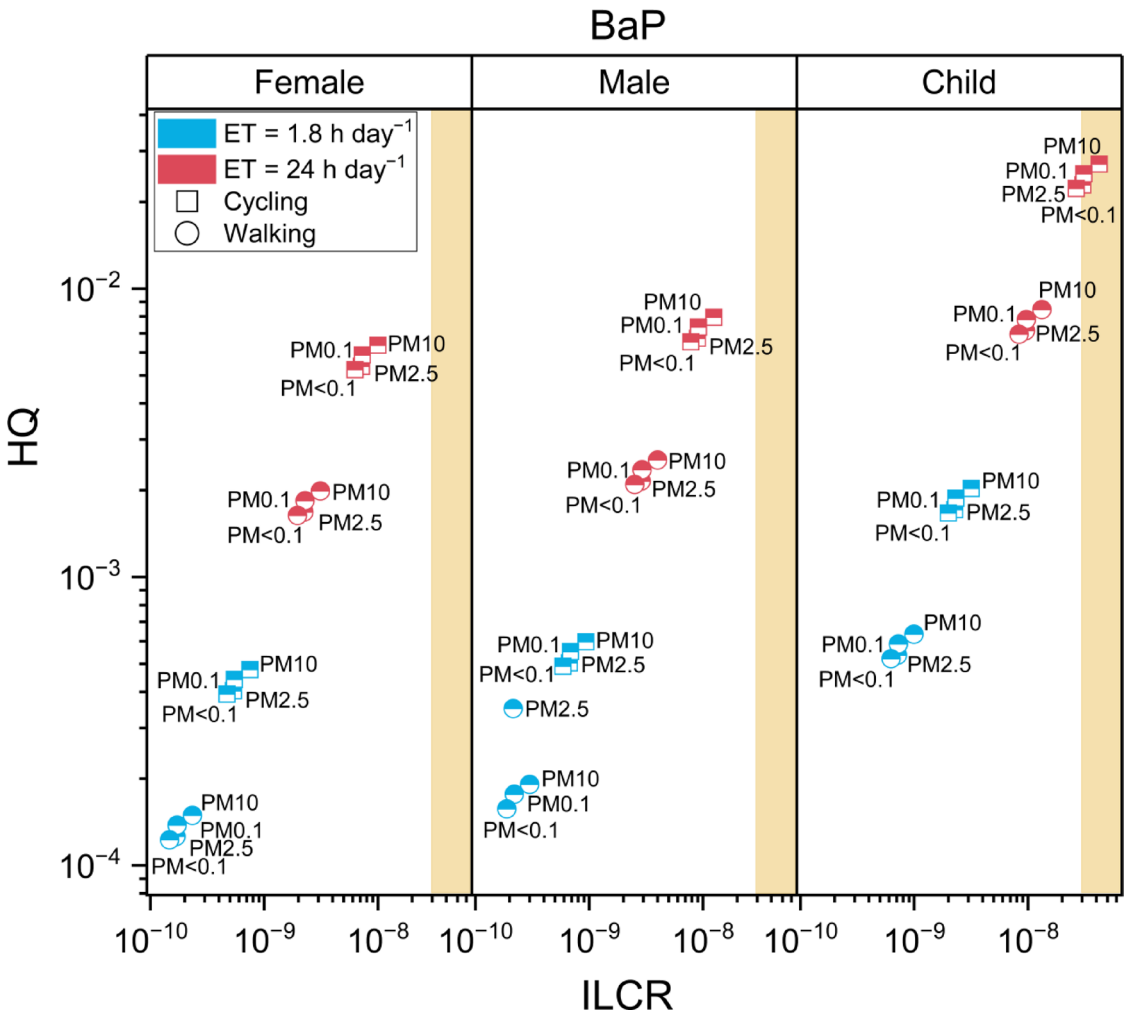

Fig. 8. The incremental lifetime cancer risk (ILCR) and hazard quotient (HQ) values associated with the inhalation of benzo(a)pyrene (BaP).

HP. The calculated HQ values were below the threshold of 1. The European PM_{10} limit values for As (6 ng m^{-3}), Cd (5 ng m^{-3}), Pb (500 ng m^{-3}), Ni (20 ng m^{-3}) and BaP (1 ng m^{-3}) were not exceeded, suggesting minimal exposure-related health risks in the study area.

These findings highlight the importance of chemical assessment of UPFs and their association with anthropogenic sources, which is essential for understanding the potential health implications and air quality status in small- and medium-sized European cities, where pollution characteristics differ from large metropolitan areas.

Data availability

Data will be made available on request from corresponding author.

Received: 4 February 2026; Accepted: 9 April 2026
Published online: 18 April 2026

References

1. Fernández-Camacho, R. et al. Ultrafine particle and fine trace metal (As, Cd, Cu, Pb and Zn) pollution episodes induced by industrial emissions in Huelva, SW Spain. *Atmos. Environ.* **61**, 507–517 (2012).
2. Morawska, L., Ristovski, Z., Jayaratne, E. R., Keogh, D. U. & Ling, X. Ambient nano and ultrafine particles from motor vehicle emissions: Characteristics, ambient processing and implications on human exposure. *Atmos. Environ.* **42**, 8113–8138 (2008).
3. Raaschou-Nielsen, O. et al. Air pollution and lung cancer incidence in 17 European cohorts: Prospective analyses from the European Study of Cohorts for Air Pollution Effects (ESCAPE). *Lancet Oncol.* **14**, 813–822 (2013).
4. Chen, H., Goldberg, M. S. & Villeneuve, P. J. A systematic review of the relation between long-term exposure to ambient air pollution and chronic diseases. *Rev. Environ. Health.* **23**, 243–297 (2008).
5. Cohen, A. J. et al. Estimates and 25-year trends of the global burden of disease attributable to ambient air pollution: an analysis of data from the Global Burden of Diseases Study 2015. *Lancet* **389**, 1907–1918 (2017).
6. Dominici, F. et al. Fine particulate air pollution and hospital admission for cardiovascular and respiratory diseases. *JAMA* **295**, 1127–1134 (2006).

7. EEA. *Air Quality in Europe — 2012 Report*. https://www.eea.europa.eu/en/analysis/publications/air-quality-in-europe-2012 (2012).
8. Gao, Y. & Ji, H. Microscopic morphology and seasonal variation of health effect arising from heavy metals in PM2.5 and PM10: One-year measurement in a densely populated area of urban Beijing. *Atmos. Res.* **212**, 213–226 (2018).
9. Fomba, K. W., van Pinxteren, D., Müller, K., Spindler, G. & Herrmann, H. Assessment of trace metal levels in size-resolved particulate matter in the area of Leipzig. *Atmos. Environ.* **176**, 60–70 (2018).
10. Ravindra, K., Sokhi, R. & Van Grieken, R. Atmospheric polycyclic aromatic hydrocarbons: Source attribution, emission factors and regulation. *Atmos. Environ.* **42**, 2895–2921 (2008).
11. Jakovljević, I. et al. Polycyclic aromatic hydrocarbons in PM10, PM2.5 and PM1 particle fractions in an urban area. *Air Qual. Atmos. Health*. **11**, 843–854 (2018).
12. Akhbarizadeh, R. et al. Suspended fine particulate matter (PM2.5), microplastics (MPs), and polycyclic aromatic hydrocarbons (PAHs) in air: Their possible relationships and health implications. *Environ. Res.* **192**, 110339 (2021).
13. Chen, Q. et al. Seasonal characteristics and health risks of PM2.5-bound organic pollutants in industrial and urban areas of a China megacity. *J. Environ. Manag.* **245**, 273–281 (2019).
14. Fadel, M. et al. PM2.5 characterization of primary and secondary organic aerosols in two urban-industrial areas in the East Mediterranean. *J. Environ. Sci.* **101**, 98–116 (2021).
15. Jedynska, A. et al. Spatial variations of PAH, hopanes/steranes and EC/OC concentrations within and between European study areas. *Atmos. Environ.* **87**, 239–248 (2014).
16. Jandacka, D., Durcanska, D. & Bujdos, M. The contribution of road traffic to particulate matter and metals in air pollution in the vicinity of an urban road. *Transp. Res. Part. D: Transp. Environ.* **50**, 397–408 (2017).
17. Mbengue, S., Alleman, L. Y. & Flament, P. Size-distributed metallic elements in submicronic and ultrafine atmospheric particles from urban and industrial areas in northern France. *Atmos. Res.* **135–136**, 35–47 (2014).
18. Khan, M. B. et al. Potential sources and meteorological factors affecting PM2.5-bound polycyclic aromatic hydrocarbon levels in six main cities of northeastern Italy: An assessment of the related carcinogenic and mutagenic risks. *Environ. Sci. Pollut Res.* **25**, 31987–32000 (2018).
19. Malandrino, M., Casazza, M., Abollino, O., Minero, C. & Maurino, V. Size resolved metal distribution in the PM matter of the city of Turin (Italy). *Chemosphere* **147**, 477–489 (2016).
20. Rogula-Kozłowska, W. et al. Spatial and seasonal variability of the mass concentration and chemical composition of PM2.5 in Poland. *Air Qual. Atmos. Health*. **7**, 41–58 (2014).
21. US EPA. *Polycyclic Aromatic Hydrocarbons (PAHs)—Integrated Risk Information System (IRIS)*. https://www.epa.gov/iris (2017).
22. WHO. *Some Non-Heterocyclic Polycyclic Aromatic Hydrocarbons and Some Related Exposures* Vol. 92 (International Agency for Research on Cancer, 2010).
23. Wise, S. A. & Watters, R. L. *Standard Reference Material 1648a—Urban Particulate Matter, Certificate Analysis*. (2020).
24. Ilenič, A., Ščančar, R. M., Đurić, M., Pranjić, A. M. & Ščančar, J. An innovative sampling device for size-fractionating airborne particulate matter for improved air pollution control of metal(oid)s and polycyclic aromatic hydrocarbons. *Anal. Methods*. **17**, 7184–7199 (2025).
25. Croghan, W. & Egeghy, P. *Methods of Dealing with Values below the Limit of Detection Using SAS*. (2003).
26. TIBCO & Statistica TIBCO Software Inc. (2017).
27. OriginLab Corporation. Origin. (2021).
28. Akyüz, M. & Çabuk, H. Gas–particle partitioning and seasonal variation of polycyclic aromatic hydrocarbons in the atmosphere of Zonguldak, Turkey. *Sci. Total Environ.* **408**, 5550–5558 (2010).
29. Caricchia, A. M., Chiavarini, S. & Pezza, M. Polycyclic aromatic hydrocarbons in the urban atmospheric particulate matter in the city of Naples (Italy). *Atmos. Environ.* **33**, 3731–3738 (1999).
30. Katsoyiannis, A., Terzi, E. & Cai, Q. Y. On the use of PAH molecular diagnostic ratios in sewage sludge for the understanding of the PAH sources. Is this use appropriate? *Chemosphere* **69**, 1337–1339 (2007).
31. Khalili, N. R., Scheff, P. A. & Holsen, T. M. PAH source fingerprints for coke ovens, diesel and gasoline engines, highway tunnels, and wood combustion emissions. *Atmos. Environ.* **29**, 1995 (1994).
32. Yunker, M. B. et al. PAHs in the Fraser River basin: A critical appraisal of PAH ratios as indicators of PAH source and composition. *Organ. Geochem.* **33**, 489–515 (2002).
33. US EPA. *Risk Assessment Guidance for Superfund Volume I: Human Health Evaluation Manual. (Part F, Supplemental Guidance for Inhalation Risk Assessment)*. (2009).
34. Republika Slovenija Statistični Urad & Prebivalstvo. https://www.stat.si/StatWeb/Field/Index/17 (2025).
35. US EPA. Exposure Factors Handbook (1997, Final Report) | Risk Assessment Portal | US EPA. https://cfpub.epa.gov/ncea/risk/recordisplay.cfm?deid=12464 (1997).
36. US EPA. *Regional Screening Level (RSL) Resident Ambient Air Table as of November 2024*. https://www.epa.gov/risk/regional-screening-levels-rsls-generic-tables (2024).
37. US EPA. *Exposure Factors Handbook (2011 Edition)*. https://www.epa.gov/expobox/exposure-factors-handbook-2011-edition (2011).
38. Agencija Republike Slovenije za okolje. ARSO vreme. (2025).
39. Valavanidis, A., Fiotakis, K. & Vlachogianni, T. Airborne particulate matter and human health: Toxicological assessment and importance of size and composition of particles for oxidative damage and carcinogenic mechanisms. *J. Environ. Sci. Health Part. C.* **26**, 339–362 (2008).
40. Gozzi, F., Ventura, G. D., Marcelli, A. & Lucci, F. Current status of particulate matter pollution in Europe and future perspectives: A review. (2017).
41. Negral, L. et al. Anthropogenic and meteorological influences on PM10 metal/semi-metal concentrations: Implications for human health. *Chemosphere* **243**, 125347 (2020).
42. Directive 2004/107/EC. *Directive 2004/107/EC of the European Parliament and of the Council of 15 December 2004 relating to arsenic, cadmium, mercury, nickel and polycyclic aromatic hydrocarbons in ambient air*. (2004).
43. US EPA. Integrated Science Assessment (ISA) for Particulate Matter (Final Report, Dec 2019). https://cfpub.epa.gov/ncea/isa/recordisplay.cfm?deid=347534 (2019).
44. Zupančič, N. Influence of climate factors on soil heavy metal content in Slovenia. *J. Soils Sedim.* **17**, 1073–1083 (2017).
45. Jiang, N. et al. Variation tendency of pollution characterization, sources, and health risks of PM2.5-bound polycyclic aromatic hydrocarbons in an emerging megacity in China: Based on three-year data. *Atmos. Res.* **217**, 81–92 (2019).
46. Schauer, C., Niessner, R. & Pöschl, U. Polycyclic aromatic hydrocarbons in urban air particulate matter: Decadal and seasonal trends, chemical degradation, and sampling artifacts. *Environ. Sci. Technol.* **37**, 2861–2868 (2003).
47. Di Vaio, P. et al. Level, potential sources of polycyclic aromatic hydrocarbons (PAHs) in particulate matter (PM10) in Naples. *Atmos. Environ.* **129**, 186–196 (2016).
48. Elzein, A. et al. A comparison of $PM_{2.5}$-bound polycyclic aromatic hydrocarbons in summer Beijing (China) and Delhi (India). *Atmos. Chem. Phys.* **20**, 14303–14319 (2020).
49. Directive 2008/50/EC. *Directive 2008/50/EC of the European Parliament and of the Council of 21 May 2008 on Ambient Air Quality and Cleaner Air for Europe*. (n.d.).

50. Alam, M. S., Delgado-Saborit, J. M., Stark, C. & Harrison, R. M. Using atmospheric measurements of PAH and quinone compounds at roadside and urban background sites to assess sources and reactivity. *Atmos. Environ.* **77**, 24–35 (2013).
51. Terzič, M. Avtomobili v EU. (2020).
52. Ono-Ogasawara, M. & Smith, T. J. Diesel Exhaust Particles in the Work Environment and their Analysis. *Ind. Health*. **42**, 389–399 (2004).
53. Tan, J. et al. Characteristics of particulate PAHs during a typical haze episode in Guangzhou, China. *Atmos. Res.* **102**, 91–98 (2011).
54. Qin, Y., Chan, C. K. & Chan, L. Y. Characteristics of chemical compositions of atmospheric aerosols in Hong Kong: Spatial and seasonal distributions. *Sci. Total Environ.* **206**, 25–37 (1997).
55. Prati, P., Zucchiatti, A., Lucarelli, F. & Mandò, P. A. Source apportionment near a steel plant in Genoa (Italy) by continuous aerosol sampling and PIXE analysis. *Atmos. Environ.* **34**, 3149–3157 (2000).
56. Thorpe, A. & Harrison, R. M. Sources and properties of non-exhaust particulate matter from road traffic: A review. *Sci. Total Environ.* **400**, 270–282 (2008).
57. Alves, C. A. et al. Polycyclic aromatic hydrocarbons and their derivatives (nitro-PAHs, oxygenated PAHs, and azaarenes) in PM2.5 from Southern European cities. *Sci. Total Environ.* **595**, 494–504 (2017).
58. Pio, C. et al. Size-segregated chemical composition of aerosol emissions in an urban road tunnel in Portugal. *Atmos. Environ.* **71**, 15–25 (2013).
59. Gaberšek, M., Watts, M. J. & Gosar, M. Attic dust: An archive of historical air contamination of the urban environment and potential hazard to health? *J. Hazard. Mater.* **432**, 128745 (2022).
60. Wilson, J. G., Kingham, S., Pearce, J. & Sturman, A. P. A review of intraurban variations in particulate air pollution: Implications for epidemiological research. *Atmos. Environ.* **39**, 6444–6462 (2005).
61. Logar, M. Izpusti delcev v zrak | Okoljski kazalci. https://kazalci.arso.gov.si/sl/content/izpusti-delcev-v-zrak-8?tid=2 (2023).
62. Statistical Office of the Republic of Slovenia. Energija za ogrevanje stanovanj in sanitarne vode. *SiStat*, https://pxweb.stat.si/SiStatData/pxweb/sl/Data/-/1815410S.px/table/tableViewLayout2/ (2026).
63. Inglič, R. T., Pirnat, U., Stare, M. & Household energy efficiency, *Statistical Office, Republic of Slovenia, 2023*. https://www.stat.si/StatWeb/en/News/Index/12783?utm_source=chatgpt.com (2024).
64. Harrison, R. M., Smith, D. J. T. & Luhana, L. Source apportionment of atmospheric polycyclic aromatic hydrocarbons collected from an urban location in Birmingham, U.K. *Environ. Sci. Technol.* **30**, 825–832 (1996).
65. Shen, R. et al. Atmospheric levels, variations, sources and health risk of PM2.5-bound polycyclic aromatic hydrocarbons during winter over the North China Plain. *Sci. Total Environ.* **655**, 581–590 (2019).
66. Li, X. et al. Wintertime aerosol chemistry in Beijing during haze period: Significant contribution from secondary formation and biomass burning emission. *Atmos. Res.* **218**, 25–33 (2019).
67. Pant, P. & Harrison, R. M. Estimation of the contribution of road traffic emissions to particulate matter concentrations from field measurements: A review. *Atmos. Environ.* **77**, 78–97 (2013).
68. Ilenič, A. et al. Determination of metal(oid)s and polycyclic aromatic hydrocarbons in size-fractionated airborne particulate matter: Methodological approaches, trends, gaps and future needs: A review. *TrEAC*. https://doi.org/10.1016/j.teac.2026.e00303 (2026).
69. Deabji, N., Fomba, K. W., dos Santos Souza, E. J., Mellouki, A. & Herrmann, H. Influence of anthropogenic activities on metals, sugars and PAHs in PM10 in the city of Fez, Morocco: Implications on air quality. *Environ. Sci. Pollut. Res.* **31**, 25238–25257 (2024).
70. Hazarika, N. & Srivastava, A. Estimation of risk factor of elements and PAHs in size-differentiated particles in the National Capital Region of India. *Air Qual. Atmos. Health*. **10**, 469–482 (2017).
71. Oroumiyeh, F. et al. Elemental composition of fine and coarse particles across the greater Los Angeles area: Spatial variation and contributing sources. *Environ. Pollut.* **292**, 118356 (2022).
72. Koçak, E., Aslan, S., İmamoğlu, İ. & Tuncel, G. Multi-group organic pollutants in urban and suburban atmospheric particulate matter (PM2.5): Temporal variation, meteorological impact, and sources. *Air Qual. Atmos. Health*. **18**, 1359–1376 (2025).
73. Canals-Angerri, A. et al. Causes of the unremitting high ambient levels of PM10 in a suburban background site in NE Spain. *Environ. Pollut*. **363**, 125113 (2024).
74. Mazziotti Tagliani, S. et al. Content, mineral allocation and leaching behavior of heavy metals in urban PM2.5. *Atmos. Environ.* **153**, 47–60 (2017).
75. Farah, E. et al. Unveiling the organic chemical composition and sources of organic carbon in PM2.5 at an urban site in Greater Cairo (Egypt): A comprehensive analysis of primary and secondary compounds. *Environ. Res.* **263**, 120118 (2024).
76. Tolis, E. I. et al. Concentration and chemical composition of PM2.5 for a one-year period at Thessaloniki, Greece: A comparison between city and port area. *Atmos. Environ.* **113**, 197–207 (2015).
77. Bandowe, B. A. M. et al. $PM_{2.5}$-bound oxygenated PAHs, nitro-PAHs and parent-PAHs from the atmosphere of a Chinese megacity: Seasonal variation, sources and cancer risk assessment. *Sci. Total Environ.* **473–474**, 77–87 (2014).
78. Hofman, J., Samson, R., Joosen, S., Blust, R. & Lenaerts, S. Cyclist exposure to black carbon, ultrafine particles and heavy metals: An experimental study along two commuting routes near Antwerp, Belgium. *Environ. Res.* **164**, 530–538 (2018).
79. Ilenič, A., Pranjić, A. M., Zupančič, N., Milačič, R. & Ščančar, J. Fine particulate matter (PM2.5) exposure assessment among active daily commuters to induce behaviour change to reduce air pollution. *Sci. Total Environ.* **912**, 169117 (2024).
80. Int Panis, L. et al. Exposure to particulate matter in traffic: A comparison of cyclists and car passengers. *Atmos. Environ.* **44**, 2263–2270 (2010).
81. Choi, E. et al. Sources of airborne particulate matter-bound metals and spatial-seasonal variability of health risk potentials in four large cities, South Korea. *Environ. Sci. Pollut. Res.* **29**, 28359–28374 (2022).

Acknowledgements

Anja Ilenič acknowledges Jožef Stefan International Postgraduate School as the institution where her PhD studies are carried out. In addition, authors would like to thank the Municipality of Maribor, Municipality of Murska Sobota, Municipality of Dobrova–Polhov Gradec, National Institute of Biology (NIB)Marine Biology Station Piran, as well as the Pavlič family (Ana, Maša, Dana, Bojan) for their valuable cooperation and assistance in installing the sampling devices.

Author contributions

AI: Writing–original draft, methodology, analysis, data curation, conceptualisation. RMŠ: Writingreview & editing, supervision, methodology, conceptualisation. AMP: Resources, project administration, funding acquisition, review & editing. NZ: Data curation, writing–review & editing. MĐ: Analysis, methodology. JŠ: Funding acquisition writingreview & editing, supervision, methodology.

Funding

This research was funded by the Slovenian Research Agency, financial support programme groups P2-0273, P1-

0143 and P1-0008, and research project J7-60124.

Declarations

Competing interests
The authors declare no competing interests.

Additional information
Supplementary Information The online version contains supplementary material available at https://doi.org/10.1038/s41598-026-48692-z.

Correspondence and requests for materials should be addressed to A.I.

Reprints and permissions information is available at www.nature.com/reprints.

Publisher's note Springer Nature remains neutral with regard to jurisdictional claims in published maps and institutional affiliations.